RL-TR-93-135
Final Technical Report
July 1993

STUDY OF MECHANISMS FOR LONG WAVELENGTH SCHOTTKY-BARRIER INFRARED DETECTORS

Rensselaer Polytechnic Institute

Leo J. Schowalter

APPROVED FOR PUBLIC RELEASE; DISTRIBUTION UNLIMITED.

Rome Laboratory
Air Force Materiel Command
Griffiss Air Force Base, New York

This report has been reviewed by the Rome Laboratory Public Affairs Office (PA) and is releasable to the National Technical Information Service (NTIS). At NTIS it will be releasable to the general public, including foreign nations.

RL-TR-93-135 has been reviewed and is approved for publication.

APPROVED:

Jerry Silverman

JERRY SILVERMAN
Project Engineer

FOR THE COMMANDER

Harold Roth

HAROLD ROTH
Director
Solid State Sciences
Electromagnetics and Reliability Directorate

If your address has changed or if you wish to be removed from the Rome Laboratory mailing list, or if the addressee is no longer employed by your organization, please notify RL (ERES) Hanscom AFB MA 01731. This will assist us in maintaining a current mailing list.

Do not return copies of this report unless contractual obligations or notices on a specific document require that it be returned.

REPORT DOCUMENTATION PAGE

Form Approved
OMB No. 0704-0188

1. AGENCY USE ONLY (Leave Blank)	2. REPORT DATE	3. REPORT TYPE AND DATES COVERED
	JULY 1993	Final

4. TITLE AND SUBTITLE
STUDY OF MECHANISMS FOR LONG WAVELENGTH SCHOTTKY-BARRIER INFRARED DETECTORS

5. FUNDING NUMBERS
C - F19628-91-K-0030
PE - 61102F
PR - 2305
TA - J1
WU - 60

6. AUTHOR(S)
Leo J. Schowalter

7. PERFORMING ORGANIZATION NAME(S) AND ADDRESS(ES)
Rensselaer Polytechnic Institute
Physics Department and Center for Integrated Electronics
Troy NY 12180

8. PERFORMING ORGANIZATION REPORT NUMBER
N/A

9. SPONSORING/MONITORING AGENCY NAME(S) AND ADDRESS(ES)
Rome Laboratory (ERES)
80 Scott Rd
Hanscom AFB MA 01731-2909

10. SPONSORING/MONITORING AGENCY REPORT NUMBER
RL-TR-93-135

11. SUPPLEMENTARY NOTES
Rome Laboratory Project Engineer: Jerry Silverman/ERES/(617) 377-4663

12a. DISTRIBUTION/AVAILABILITY STATEMENT
Approved for public release; distribution unlimited.

12b. DISTRIBUTION CODE

13. ABSTRACT (Maximum 200 words)

We have studied ballistic electron transport across metal layers and metal/semiconductor interfaces using a scanning tunneling microscope to inject electrons with a controlled energy into a thin metal film, allows measurements (with spatial resolution approaching 1nm) of (i) the local Schottky barrier (SB) height, (ii) ballistic mean free paths of energetic electrons (or holes), and (iii) transmission probability of hot carriers across the metal/semiconductor interface. The attenuation length of hot electrons (1.5 eV above the Fermi level) in PtSi is measured as approximately 4 nm. We also used BEEM to observe the sharp onset of inelastic scattering mechanisms in Au/Si and PtSi. We observe that the derivative BEEM spectrum of Au/Si (001) n-type is rich with features which may correspond to either M/S interface states or to states in the semiconductor bandgap near the interface. We suggest that these interface scattering processes occur also for other M/S systems. Our experimental BEEM studies indicate that hot electron transport is diffusive in the sense that electrons will scatter elastically many times before an inelastic event will occur. We succeeded in constructing a low temperature (liquid nitrogen temperatures) BEEM head and have taken BEEM spectra of PtSi on P-type Si.

14. SUBJECT TERMS	15. NUMBER OF PAGES
Ballistic-electron-emission microscopy (BEEM), Schottky-barrier PtSi, Hot carriers Infrared Detectors	32
	16. PRICE CODE

17. SECURITY CLASSIFICATION OF REPORT	18. SECURITY CLASSIFICATION OF THIS PAGE	19. SECURITY CLASSIFICATION OF ABSTRACT	20. LIMITATION OF ABSTRACT
UNCLASSIFIED	UNCLASSIFIED	UNCLASSIFIED	UL

Abstract -

During this contract, we have studied ballistic electron transport across metal layers and metal/semiconductor interfaces using ballistic-electron-emission microscopy (BEEM). This new technique, which uses a scanning tunneling microscope to inject electrons with a controlled energy into a thin metal film, allows measurements (with spatial resolution approaching 1 nm) of (i) the local Schottky barrier (SB) height, (ii) ballistic mean free paths of energetic electrons (or holes), and (iii) transmission probability of hot carriers across the metal/semiconductor interface. We have measured the attenuation length of hot electrons (1.5 eV above the Fermi level) in PtSi to be approximately 4 nm. The SB height of PtSi on n-type Si (as determined by BEEM) is 0.87 eV, in good agreement with optical measurements. We have also used BEEM to observe the sharp onset of inelastic scattering mechanisms in Au/Si and in PtSi/Si. We experimentally demonstrated, for the first time, that the creation of electron-hole pairs near the metal/semiconductor (M/S) interface significantly affects the scattering of the ballistic electrons with energy greater than the semiconductor substrate energy gap. In addition, we observe that the derivative BEEM spectrum of Au/Si(001) n-type is rich with features which may correspond to either M/S interface states or to states in the semiconductor bandgap near the interface. We suggest that these interface scattering processes occur also for other M/S systems. Our experimental BEEM studies indicate that hot electron transport is diffusive in the sense that electrons will scatter elastically many times before an inelastic event will occur. We have demonstrated, for the first time, ac BEEM which was found to give a linear threshold for the Schottky barrier, and it also clearly showed the onset of electron-hole pair creation and other inelastic scattering events. We have also succeeded in constructing a low temperature (liquid nitrogen temperatures) BEEM head and have succeeded in taking BEEM spectra of PtSi on p-type Si. It is our belief that these studies of ballistic carrier transport will allow a fundamental determination of how to achieve higher quantum efficiencies in Schottky-Barrier Infrared Detectors.

Introduction

While the technology of Schottky barrier infrared detectors (SBIRDs) on silicon substrates is fairly advanced, details about the ballistic propagation of photoexcited electrons or holes to the metal/semiconductor (m/s) interface and the probability of transmission across the m/s interface are not well understood. Scattering mechanisms in the metal layers for carriers with energies a few tenths of an eV above the Fermi level are not well understood. In addition, the energy dependence of the quantum mechanical reflection, which must occur at the Schottky barrier (SB) between the metal and semiconductor, is generally ignored. The details of the band structure and the effects of defects are included only phenomenologically, if at all, since the experimental studies of these details have been difficult. In the past, the development of SBIRDs has proceeded largely by trial and error with some clever physical insight but little hard information. In addition, the development of new m/s interfaces with potentially lower SB heights and with improved transmission coefficients has been slowed by the requirement that high quality, uniform interfaces be created over large areas before the photoresponse can be properly tested. A technique that allows the testing of ballistic transmission of hot holes (or electrons) across very small regions which are likely to be defect free would enable the exploration of many more potentially interesting m/s interfaces. The materials development efforts (which generally are costly and time consuming) could then be invested in only those systems which have demonstrated intrinsically high transmission coefficients in the right wavelength range.

Here, we report on our studies of ballistic electron transport in Au/Si and in PtSi/Si using ballistic-electron-emission microscopy (BEEM). This new microscopy technique uses a scanning tunneling microscope (STM) to inject electrons with a controlled energy into a thin metal film. BEEM allows measurements (with spatial resolution approaching 1 nm) of (i) the local SB height, (ii) ballistic mean free paths of energetic electrons (or holes), and (iii) transmission probability of hot carriers across the m/s interface. We have also begun work depositing SiGe alloys on Si substrates to study ways to create lower SB heights for use further into the infrared.

In ballistic-electron-emission microscopy (BEEM) and in ballistic-electron-emission spectroscopy (BEES), the scanning-tunneling microscope (STM) tip functions as an emitter of electrons which tunnel across a vacuum energy barrier into a base region consisting of a thin metal overlayer on a collector region consisting of a semiconductor. An extra connection is provided to the STM so that contacts are made to the STM tip, the thin metal layer, and the semiconductor substrate. The STM becomes a three terminal device similar to a transistor. The operation of BEEM is shown in a schematic energy diagram shown in Fig. 1. By injecting electrons over a local base region and changing the STM tip-to-sample bias, one does BEES, and by holding the bias voltage constant and scanning the STM tip over the metal base, one does BEEM. By using BEES, one can study the energy dependence of carrier transport within the metal base and across the metal/semiconductor (m/s) interface. By using BEEM, one can study the spatial variation of the Schottky barrier height and of transport across the metal base and across the m/s interface.

Imaging the metal/semiconductor interface with BEEM

The superior spatial resolution of STM suggests that the spatial resolution of BEEM may be excellent. The initial study in BEEM promised a superior spatial resolution of 1-2 nm by BEEM for a 5-nm-thick metal overlayer [1]. This spatial resolution requires that the injected electron beam remains ballistic in the metal base, i.e. no elastic scattering occurs and all inelastic scattering takes away enough energy to thermalize the electrons. This requirement contradicts the findings from experiments using internal photoemission that discovered inelastic mean free path to be much longer than the elastic mean free path length in many metals including Au. [2] It also contradicts the theoretical estimates on the inelastic mean free path of electrons. [3] If, as the theory predicts, the inelastic mean free path length is approximately 100 nm for an electron 1 eV above the Au Fermi level, then an electron injected into a 5-nm-thick metal base will scatter elastically many times before it thermalizes, and the spatial resolution of BEEM will be on the order of 10 nm.

It is important, however, to distinguish between the experimentally observed spatial resolution and the spatial resolution for the ideal cases. If there are strongly scattering defects such as a domain boundary, then sharp contrasts may be seen in the BEEM images across a grain boundary, even though the intensity within each grain may be uniform. This effect may have been observed by Niedermann *et al.* [4] It is important to realize that the spatial resolution of BEEM is not the same everywhere, that the ideal case in which the metal overlayer is single crystal has limited applications because defects such as grain boundaries are not included.

A pair of STM and BEEM images is shown in Fig. 2. These images were taken from a sample consisting of 100 Å of Au on Si(001) n-type. The STM image shows a large step running diagonally and a large island of Au on one side of it. The BEEM image shows a large drop in the BEEM current over the Au island, and it also shows a large drop which appears uncorrelated with any surface feature. It was expected that the BEEM current would decrease over the Au island, since the injected electrons from the STM tip has to travel a longer distance over a thicker portion of the Au overlayer. What is perhaps surprising is that the drop in the BEEM current is so sudden, and also that the "search-light effect" is not evident over the Au island edge. The BEEM current is nearly uniform within regions which are sharply defined by 1-2 nm.

To get a more precise measure for the manifestation or the absence of the search-light effect, individual lines from the region shown in Fig. 2 were examined. In Fig. 3 is shown a plot of the surface tilt-angle from the surface normal calculated from a line scan, and also a plot of the BEEM current over the same line. Ten line scans were averaged to decrease the noise in the BEEM current. As in Fig. 2, it is seen in Fig. 3 that: (1) the drop in the BEEM current is sudden, and (2) the search light effect is not present.

A test of the claim that electron transport is ballistic in the metal overlayer is the evidence for

or the lack of the "search-light effect." This effect arises because the tunneling electron distribution from the STM tip is sharply peaked about the surface normal of the metal base. If the metal surface is tilted with respect to the semiconductor substrate, then the injected electrons will have to travel further than the thickness of the metal overlayer to reach the m/s interface, the distance being greater if the tilt angle is greater. In the ballistic regime where there is no elastic scattering, this effect should be noticeable, whereas, in the diffusive regime, this effect should not be seen. We used the planar tunneling model (based on WKB approximation for a trapezoidal barrier) as is commonly done, and we feel justified in using it since a more sophisticated s-wave model by Tersoff gives nearly the same momentum distribution of the tunneling electrons. [5] The absence of the search-light effect supports our earlier Monte Carlo simulation [6] in indicating that the transport in Au base is diffusive. Diffusive here means that the hot electrons will undergo many elastic (or "quasi-elastic") scattering events before undergoing an inelastic scattering event which will cause the electron to lose sufficient energy so as to be unable to cross the Schottky barrier.

Ballistic-electron-emission spectroscopy (BEES)

Figure 4 shows a BEEM spectrum from a data set in which the tip bias voltage, with respect to the grounded Au (on Si(001) n-type), ranges from -400 to -1700 mV. The data set is an average of 500 scans from which a linear function is subtracted to best give zero BEEM current for data points more than 0.1 eV below the Schottky barrier threshold. Each BEEM spectrum consisted of 131 points gotten by ramping the STM tip bias voltage down from -400 to -1700 in -10 mV steps, ramping it up from -1700 mV to -400 mV in +10 mV steps, and then averaging the two BEEM signal readings at each of the STM tip bias voltages. Because of the low-pass filter, the STM tip bias voltage ramp rate was limited to about 2 Hz to allow the transient electrical responses to decay. Given this data acquisition rate, it took 3-4 hours to take one hundred BEEM spectra, and small variations in the ambient temperature during the data acquisition inevitably resulted in some thermal drift. In our experiment, the STM tip was allowed to drift over relatively large areas so that an averaged BEEM spectrum represents a spatial average. It is entirely possible that the BEEM spectra taken has spatial variations that can be correlated with surface features such as steps, terraces, domain boundaries, and defects, but the experimental difficulty of localizing the STM tip for hours on any of those features is formidable --- an extremely thermally stable STM, a very large signal to noise ratio, a new and faster BEEM technique, or a combination of these will be necessary to do such an experiment. It is our intention to pursue these possibilities in the follow-on contract.

To fit our data, we use an extension of the original BEEM theory by Bell and Kaiser[9]. We have shown [7] that the similarity of the BEEM spectra for Au/Si(001) and Au/Si(111) necessitates the extension of the theory to include the effects of scattering in the metal overlayer and near the M/S interface. In our theory, the BEEM current is given by the following equation:

$$I(V) = \alpha \frac{\int_0^\infty dE_x D(E_x) \int_0^\infty dE_t f(E)\,(1-\cos(\theta_c))\,H(E-eV-E_t-\phi_s)\,G(V)}{2\int_0^\infty dE_x D(E_x) \int_0^\infty dE_t (f(E)-f(E-eV))} \qquad (1)$$

where I is the BEEM current, V is the tip bias voltage with respect to the sample, e is the free electron charge, E_x and E_t are the kinetic energies of the electrons in the STM tip associated with the normal and the parallel components of the wave vector, E is the sum of E_x and E_t, f is the Fermi-Dirac distribution, D is the WKB tunneling probability for a planar trapezoidal barrier, H is the Heavyside step function, E_F is the Fermi energy of the metal overlayer, ϕ_S is the Schottky barrier height, α is an adjustable parameter, and θ_c defines the critical angle cone for the collection at the Schottky barrier maximum.

$$\cos(\theta_c) = \left(\frac{\phi_s + E_f}{E - eV}\right)^{0.5} \qquad (2)$$

Two implicit parameters in $D(E_x)$ are the tip to the sample separation s and the work function ϕ_w of the metal tip. For the fit shown in Fig.4, we assumed that s = 5 Å, ϕ_w= 3 eV, E_f = 5.4 eV, because these are realistic values expected during the STM operation. We performed a least square fit of the data shown in Fig. 4 to our theory with ϕ_S and α as variables, and computed χ^2 to determine the range of good fit values for ϕ_S and found it to be 780 ± 10 meV. The assumptions used to fit the BEEM spectrum threshold have been used successfully by others (and are used here) even though Stiles and Hamann [10] have pointed out that a variation in the STM tip to the sample separation as a function of the STM tip bias voltage may be significant and will indeed affect the fitting parameters ϕ_S and α. The main point of doing the fit was to emphasize the necessity of introducing the function $G(V)$ in Eq. (1). It will be explained later that $G(V)$ is necessary to describe the sudden onset of inelastic scattering in the high energy portion of the BEEM spectrum.

In deriving the above equations, we assumed that sufficient elastic scattering occurs in the metal overlayer or at the interfaces to cause a complete momentum relaxation of the hot electrons, resulting in an isotropic momentum distribution in the metal overlayer. We also assumed that the energy is conserved, and that an electron can contribute to the BEEM current only if it lies within the critical angle cone defined by θ_c. These assumptions are supported by our earlier Monte Carlo simulation [7] of the elastic and the inelastic scattering in the Au and at the interfaces. The assumption of the strong elastic scattering is expected to be very good for Au/Si because of the rapid mixing of Au and Si and the roughness of the Au/Si interface[11], and because of the long inelastic mean free path length for Au [12]. The use of the WKB approximation for a planar trapezoidal tunnel barrier is justified because a more sophisticated theory[5], taking into account the nonplanar shape of the STM tip, gives a

similar tunneling electron distribution.

Fig. 5 shows the derivative BEEM spectrum made from the same data set used for Fig.4 by doing least square fit of a quadratic function to five consecutive data points and calculating the derivative with this function. The low noise in the data set and the fine sampling of the BEEM current at 10 mV intervals allowed the differentiating procedure to give the derivative spectrum in which several new features previously unidentified in the Au/Si BEEM spectrum are prominent. Prior BEEM theories[7,9,13] predict that the BEEM spectrum behaves like a thermally broadened square or a 5/2 power function near the threshold, and that it slowly becomes linear and sublinear at high energies. Fig. 5 shows that, contrary to theoretical expectations, there is a sharp high energy threshold at 1040 mV, and also that there are other interesting features. At this time, we have examined many samples for this study and taken thousands of BEEM spectra, and all the averaged spectra from the subsets examined by us show the same sharp high energy threshold, although they vary in some of the other features. An interpretation of this feature is that 1040 mV marks the opening of the scattering channel for the exciton creation to occur at the Au/Si(001) n-type interface. Energetically, an electron of energy 1040 meV above the Au Fermi sea is not allowed to form an exciton, but an optical phonon in Si, which has energy of about 60 meV on the average[14], can assist the creation of an exciton, which has binding energy of 14.7 meV [15]. At energies higher than 1120 meV, incident electrons are energetically allowed to form electron-hole pairs without phonon assistance, and this opens another reaction channel. The two reactions discussed so far must occur near the Au/Si(001) interface for the incident electron to have an available final state either above the metal Fermi sea or into one of the unoccupied Au/Si interface states. One should expect a square law rate for the electron-hole pair creation at the M/S interface by an argument similar to that for the electron-electron scattering[16]. This process is put into our BEEM theory by the introduction of the function G in Eq. (1) defined as follows.

$$G(V) = 1 - \beta H(E - eV - E_f - E_{gap})\,(E - eV - E_f - E_{gap})^2 \quad , \qquad (3)$$

where E_{gap} is the semiconductor energy gap, and β is an adjustable parameter. For the fit shown in Fig. 4, α = 2.66 and $\beta = 2.61 \times 10^{-2}$. Fig. 4 shows that our theory fits the data well over the entire range of the BEEM spectrum. Our theory explains the high energy roll-off of the Au/Si BEEM spectrum, and reconciles the published BEEM data for Au/GaP[13], which show no appreciable roll-off up to 2 eV (GaP has bandgap of 2.5 eV), with the data for Au/Si[17], which show significant roll-off by 2 eV. Our theory implies that, just as the electron-electron scattering in the metal overlayer contributes to the reverse BEEM current, the electron-hole pair creation also contributes. The published reverse BEEM data for Au/Si(001) n-type at 77 K shows a discrepancy between the reverse BEEM theory and the data in the high energy regime[16]. We suggest that this is due to the electron-hole pair creation near the Au/Si interface followed by its decay into the Si leading to the contribution of an electron to the BEEM current.

In addition to the features around the Si energy gap, the derivative BEEM spectrum also shows other features due either to the Au/Si interface states or to the states in Si energy bandgap. Fig. 6 shows four derivative BEEM spectra taken from the same sample at different locations of Au/Si(001). Each spectrum is an average of 100 spectra and was calculated as described for Fig. 5. Common features, apparently due to the openings of reaction channels at 1040 meV, at 1120 meV, and at 1230 meV are noted. Some of the sharp features in Fig. 6, one near 1350 mV for example, are less apparent in the average of a larger set of data shown in Fig. 5, and this implies that these features are present only in a fraction of the BEEM spectra, perhaps as a result of the thermal drift described earlier. The fact that the sharp features seen in the average of 500 BEEM spectra shown in Fig. 5 are also apparent in each of four averages of 100 BEEM spectra shown in Fig. 6 rules out infrequent noise in the BEEM signal as the cause of these features. The exact location of the peaks shift by 0-30 mV from spectrum to spectrum, and this is probably caused either by the sensitivity of the derivative spectra to noise in the data or by a spatial dependence of these features.

Unambiguous interpretation of the peak at 1230 meV and other features apparent in Fig. 5 and Fig. 6 are difficult for the Au/Si interface because it is relatively complex; Au and Si mixes across the interface in time, Au is known to create deep impurity levels in Si bandgap[18], Si has intrinsic interface states[19], and Au may create interface defect states. The observed features should not be due to states in the metal overlayer, because the Au density of states is smooth near its Fermi level. As discussed below (in the ac BEES Section), studies of PtSi/Si show that its derivative BEEM spectrum also contains several sharp features, and that it has just as strong a threshold due to the exciton creation as Au/Si(001). This implies that the electron-hole pair creation is universal (preliminary studies of $CoSi_2$ have also shown this effect) to ballistic electron transport across m/s interfaces.

In conclusion, we have demonstrated that the roll-off of the Au/Si BEEM spectrum at energies well above the Schottky barrier threshold is predominantly due to electron-hole pair creation. Other features are observed in the derivative BEEM spectrum which we believe are due to the onset of other inelastic scattering processes. These findings reconcile some of the previously unexplained observations in other BEEM experiments, and we suggest that the derivative BEEM spectroscopy should be used to reexamine other M/S systems such as PtSi/Si and PtSi/SiGe. The combination of BEEM's excellent spatial resolution and the good energy resolution demonstrated here for Au/Si proves BEEM to be a powerful technique for studying the electron and the hole scattering at the M/S interface in general and, in particular, for determining the effects of the interface states and the localized defects.

ac Ballistic-electron-emission spectroscopy (ac BEES)

An ac BEES spectrum for our Au/Si sample is shown in Fig. 7. The spectrum can be compared to the derivative of a dc BEES spectrum shown in Fig. 5, and it is found that the ac BEES spectrum shows less noise below the Schottky barrier energy. The dc BEES spectrum and the ac BEES spectrum are both averages of many spectra taken over a few hours. Each

spectrum that was averaged consisted of many data points, and the dc BEES data points were taken at a rate of few Hz while the ac BEES data points were taken at a few tenth of Hz. The quality of the ac BEES spectrum demonstrates that the signal-to-noise ratio of each data point was better than for the conventional dc BEES. This can be understood in terms of the noise bandwidth. In dc BEES, the noise bandwidth was approximately 10 Hz due to the passive low pass filter that we used. In ac BEES, the lock-in detects only the reference frequency within the precision of the amplifier. In our case, the bandwidth of the lock-in was set at 1 Hz (determined by the output filters of the phase-sensitive detectors and as a compromise between narrowing the bandwidth and increasing the data acquisition time) and hence ac BEES data has at least ten times the signal-to-noise ratio of dc BEES data, presuming that the power spectral density of noise is nearly flat or behaves like 1/f below 10 Hz.

An ac BEES spectrum of Au/PtSi/Si is shown in Fig. 8. For PtSi layer 50 Å thick, the BEES signal was approximately 1/5 that of Au/Si with same thickness of Au overlayer and this makes the ac BEES spectrum appear noisier, but the major features such as the Schottky barrier height and the onset of electron-hole pair creation can still be read easily from the figure. The lower BEEM current was due, in part, to the shorter attenuation length of electrons in PtSi as described in the next Section.

There are several methods of doing ac BEES, but the simplest uses the constant tunnel current mode. In this method, the tunnel current is maintained to be constant, and the BEEM current is the following function of time.

$$I_{ac}(t) = I(V_{dc} + V_o e^{i\omega t}) + N(t) \quad , \tag{4}$$

where V_o is the amplitude of the ac modulation, ω is the angular frequency of ac modulation, V_{dc} is the STM tip bias voltage to which the ac modulation is added, I is the dc BEEM spectrum, and $N(t)$ is noise. The Fourier component of the BEEM signal at ω is

$$I(\omega) = F.T.[I_{ac}(t)] = \frac{1}{T}\int_o^T I(V_{dc} + V_o e^{i\omega t})\, e^{-i\omega t} dt \quad , \tag{5}$$

where $F.T.$ denotes the operation of Fourier Transform and T is the finite time interval of integration. It can be shown rigorously [20] that

$$I(\omega) = V_o \frac{\partial I}{\partial V}\Big|_{V=V_{dc}} \quad , \tag{6}$$

The lock-in measures the RMS value of the signal at the lock-in frequency, and this is equal to $|I(\omega)|/\sqrt{2}$.

There are several advantages to doing ac BEES. First, the ac BEES spectrum, being same as the derivative of the dc BEES spectrum, shows energy dependent features much clearer than the dc BEES spectrum. For example, the Schottky barrier height can be easily determined by linear interpolation of a portion of the ac BEES spectrum just above the threshold, instead of relying on time consuming fit routines which are model-dependent. Furthermore, the linearity of the Schottky barrier threshold allows easy detection of deviation from it, such as the opening of higher energy threshold due to the creation of electron-hole pairs at the m/s interface at the energy of 1040 meV. Higher doping of the semiconductor substrate may increase the effect of quantum mechanical reflection (QMR) to change the linear threshold to 3/2 power [21], but at 10^{15} cm^{-3} or less the energy dependence of QMR is expected to be significantly weakened by phonon scattering in the semiconductor [22]. Impact ionization in the semiconductor depletion region [23] and electron-electron interaction in the metal [13] modify the dc BEES spectrum at high STM tip bias, and these will be also more apparent in the ac BEES spectrum.

Another advantage of ac BEES is that the signal frequency can be high, and this allows the potential for faster data acquisition and also for taking data in a frequency range where there is a minimum amount of noise. For example, one may decide to use 1 kHz as the ac modulation frequency; at that frequency, the 1/f noise is negligible, and data can be taken at a few hundred Hz rate. In our case, ac BEES could not be done at high frequency due to a capacitive coupling between the STM tip wires and the BEEM signal wires and also due to the small bandwidth of our amplifiers. However, both of these problems are specific to the experimental setup used, and they can be significantly reduced in principle by shielding and by using higher harmonics of the reference signal.

Determination of the attenuation of hot electrons in PtSi

The attenuation length of electrons in PtSi was determined by making measurements on three different Au/PtSi/Si (n-type) samples with 0, 50, and 100 Å thicknesses of PtSi. The magnitude of the BEES current showed a simple exponential PtSi-thickness dependence with an attenuation length of 4 nm. A plot of this data along with the fitted attenuation length is shown in Fig. 9. We are planning to complete attenuation length measurements of hot holes in PtSi on p-type Si on the follow-on contract.

Growth of SiGe alloys in the Si MBE system

We completed reconfiguration of our Si MBE chamber so that we are now able to deposit SiGe alloys followed by PtSi deposition in the same UHV chamber. We have begun work on this project and have shipped some of the SiGe samples to Dr. Jimenez at Rome Laboratory for Schottky barrier testing. Problems, however, with the Inficon Sentinel, which is being used to control the rate of metal deposition, prevented us from doing much experimental

work on this system during the current contract. It will be pursued further in the follow-on contract.

Low temperature BEEM measurements

As indicated in our proposal, it is necessary to make BEEM measurements of PtSi on p-type Si at liquid nitrogen temperatures because the low Schottky barrier height results in too low an effective resistance between the metal layer and the semiconductor substrate at room temperature. To make these measurements, we have constructed a new STM head which is designed to function in a liquid nitrogen bath. In addition, we have constructed a dry box which houses the microscope and the liquid nitrogen bath. The dry box was required to avoid condensation of water vapor in addition to protectecting the surface of reactive samples. This part of the project was completed during the summer of 1992, however, problems with the microscope prevented us from being able to immediately take useful BEEM data. We have been able to solve these problems and have now started taking BEEM data on PtSi on p-type Si. Initial results are shown in Fig. 10 which is a BEES spectrum taken with tunnel current of 0.9 nA. It is an average of 100 files, and no offset subtraction nor smoothing was done. The PtSi sample was supplied by Dr. Jimenez from Rome Laboratory and consisted of 5 nm of PtSi on Si(001) p-type. We then deposited 5 nm of Au on top of the PtSi layer. From the fit, the Schottky barrier height comes out to be 0.28 eV. This seems unreasonably high when compared with photoresponse measurements. We are presently in the process of determining the cause of this high barrier height. At least one possibility is that the sample was damaged in the initial BEEM measurements. Another is that there is significant spatial variation of the Schottky barrier height which, of course, would be of great interest.

Papers published (or submitted) acknowledging this Contract

"Electron-hole pair creation and metal/semiconductor interface scattering observed by ballistic-electon-emission microscopy," E.Y. Lee and L.J. Schowalter, Phys. Rev. B15 (Rapid Communication) **45**, 6325 (1992).

"Fundamental studies of Schottky barrier infrared detectors by ballistic-electron-emission microscopy," L.J. Schowalter, E.Y. Lee, B.R. Turner, and J.R. Jimenez, **Infrared Focal Plane Array Producibility and Releated Materials**, ed. R. Balcerak, P.W. Pellegrini, D.A. Scribner (SPIE Proc. Vol. 1683, 1992) p. 152.

"Imaging of metal/semiconductor interface by ballistic-electron-emission microscopy (BEEM)", E.Y. Lee, B.R. Turner, J.R. Jimenez, and L.J. Schowalter, submitted to MRS Proc., Fall MRS Meeting, Boston, Dec., 1992.

"Diffusive and inelastic scattering in ballistic-electron-emission spectroscopy and ballistic-electron-emission microscopy," E. Y. Lee, B. R. Turner, L. J. Schowalter, J. R. Jimenez, submitted to J. Vac. Sci. Technol. (1993).

Thesis submitted which achnowledged this Contact

E.Y. Lee, **Study of BallisticCarrier Transport using Ballistic-Electron-Emission Microscopy** (Ph.D. thesis, Rensselaer Polytechnic Institute, 1992) unpublished.

References

[1] W. J. Kaiser and L. D. Bell, Phys. Rev. Lett. **60**, 1406 (1988).
[2] R. N. Stuart, F. Wooten, and W. E. Spicer, Phys. Rev. Lett. **10**, 7 (1963).
[3] J. J. Quinn, Phys. Rev. **126**, 1453 (1962); J. J. Quinn, Appl. Phys. Lett. **2**, 167 (1963).
[4] P. Niedermann, L. Quattropani, K. Solt, A. D. Kent, O. Fischer, J. Vac. Sci. Tech. B **10**, 580 (1992).
[5] J. Tersoff (unpublished).
[6] E. Y. Lee and L. J. Schowalter, Phys. Rev. B15, **45**, 6325 (1992).
[7] L. J. Schowalter and E. Y. Lee, Phys. Rev. B15, **43**, 9308 (1991).
[8] R. T. Tung, A. F. Levi, J. P. Sullivan, and F. Shrey, Phys. Rev. Lett. **66**, 72 (1991).
[9] L. D. Bell and W. J. Kaiser, Phys. Rev. Lett. **61**, 2368 (1988).
[10] M. D. Stiles and D. R. Hamann, Phys. Rev. Lett. **66**, 3179 (1991).
[11] L. J. Brillson, A. D. Katnani, M. Kelly, and G. Margaritondo, J. Vac. Sci. Technol. A **2**, 551(1984).
[12] R. N. Stuart, F. Wooten, and W. E. Spicer, Phys. Rev. Lett. **10**, 7 (1963).
[13] M. Prietsch, and R. Ludeke, Phys. Rev. Lett. **66**, 2511 (1991); R. Ludeke, M. Prietsch, A. Samsavar, J. Vac. Sci. Technol. B **9**, 2342 (1991).
[14] B. N. Brockhouse, Phys. Rev. Lett. **2**, 256 (1959).
[15] N. O. Lipari and A. Baldereschi, Phys. Rev. B **3**, 2497 (1971).
[16] L. D. Bell, M. H. Hecht, W. J. Kaiser, and L. C. Davis, Phys. Rev. Lett. **64**, 2679 (1990).
[17] H. D. Hallen, A. Fernandez, T. Huang, R. A. Buhrman, and J. Silcox, J. Vac. Sci. Technol. B **9**, 585 (1991).
[18] S. M. Sze, **Physics of Semiconductor Devices** (John Wiley & Sons, New York, 1981), p. 21.
[19] J. A. Stroscio, R. M. Feenstra, and A. P. Fein, Phys. Rev. Lett. **57**, 2579 (1986).
[20] E. Y. Lee, Ph. D. thesis (Rensselaer Polytechnic Institute, 1992) unpublished.
[21] A. M. Milliken, S. J. Manion, W. J. Kaiser, L. D. Bell, and M. H. Hecht, Phys. Rev. B **46**, 12826 (1992).
[22] E. Y. Lee and L. J. Schowalter, J. Appl. Phys. **70**, 2156 (1991).
[23] R. Ludeke, J. Vac. Sci. Tech. (to be published) (1993).

Figure Captions

Fig. 1: In BEEM, the STM tip functions as an emitter of electrons, some of which travel across the thin metal base and across the metal/semiconductor interface into the semiconductor collector.

Fig. 2: A scanning tunneling microscope (STM) image and the corresponding BEEM image is shown for 10 nm of Au evaporated on Si(001) n-type. The tunnel current was 0.9 nA, and the scanned area was 35×35 nm^2.

Fig. 3: The experimentally measured tilt angle and the BEEM current is shown for a line scan across the region shown in Fig. 2. As explained in the text, the search-light effect is not seen.

Fig. 4: A BEEM spectrum averaged from 500 experimental BEEM spectra taken at 0.9 nA constant tunnel current on a 7 nm thick Au/Si(001) n-type is shown with a theoretical fit using Eq. (1). Only every fifth point, from the original data set of 131 points, is shown.

Fig. 5: The derivative BEEM spectrum of the data shown in Fig. 4, calculated as described in the text, is shown. A sharp threshold about the energy gap of Si at 1.12 eV is apparent, as are other interesting features.

Fig. 6: Four derivative BEEM spectra are shown which are taken from different subsets of the experimental data set. These spectra show that there are common features in the derivative BEEM spectra that we propose are associated with the creation of electron-hole pairs and also with other inelastic scattering processes occurring near the metal/semiconductor interface.

Fig. 7: An ac BEES spectrum of Au/Si(001) n-type is shown. The ac modulation amplitude was 10 mV RMS. The linear Schottky barrier threshold starting at 800 mV and also other features at higher energies are easily seen, in contrast to the conventional dc BEES spectrum.

Fig. 8: An ac BEES of Au/PtSi/Si(001) n-type is shown. Similar features as Au/Si are seen, but some details are distinct. The smaller BEES signal makes the spectrum appear noisier.

Fig 9: The attenuation of the BEEM current in Au/PtSi/Si(001) n-type is shown as a function of the PtSi thickness. The thickness of the Au layer was always 5 nm and the STM tip bias voltage was -1.5 V with respect to the sample. The tunnel current was kept fixed at 0.9 nA. A fit, assuming an exponential relationship, is also shown.

Fig. 10: A BEEM spectra of Au/PtSi/Si (p-type) is shown which was taken at 77 K. A complete description of how the spectrum was taken is given in the text.

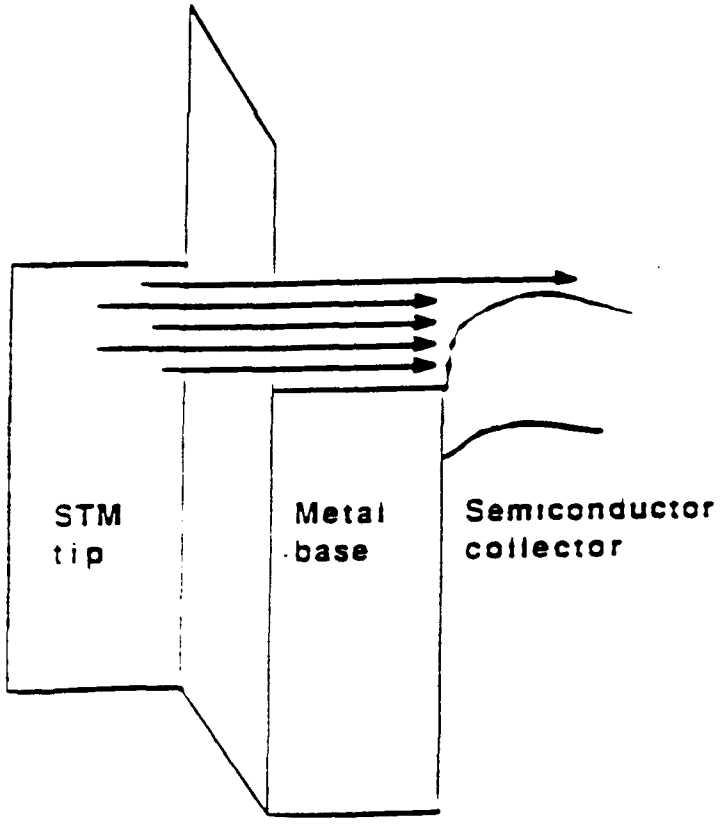

Fig. 1

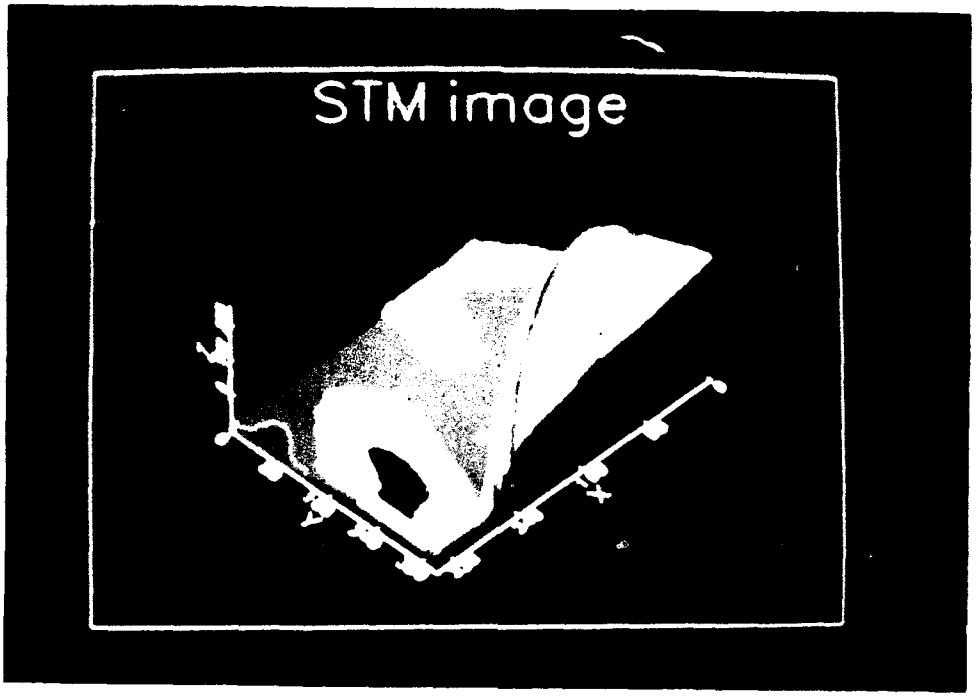

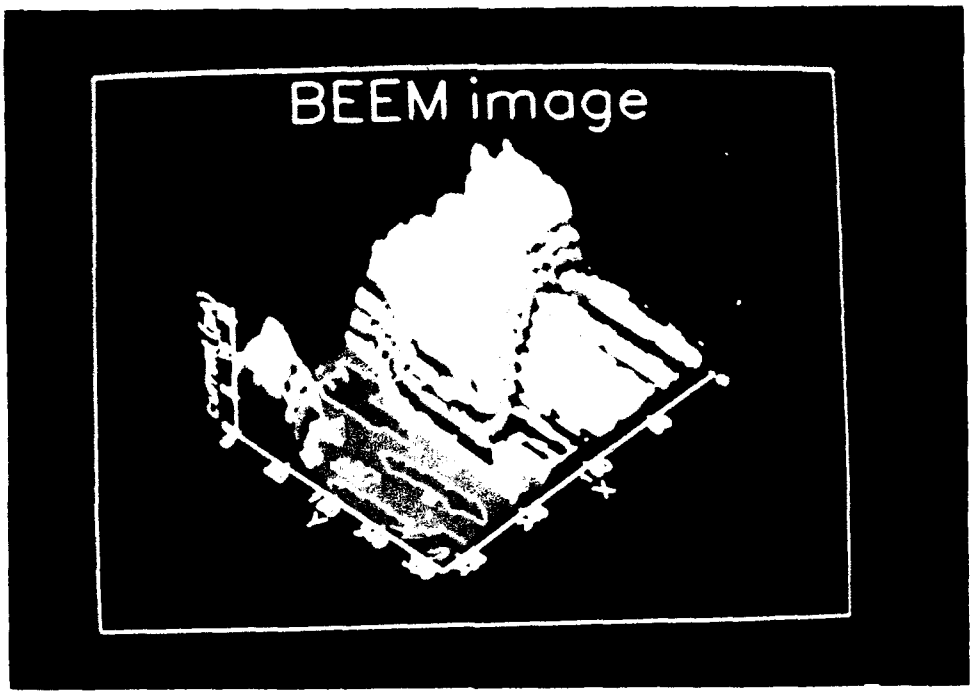

Fig. 2

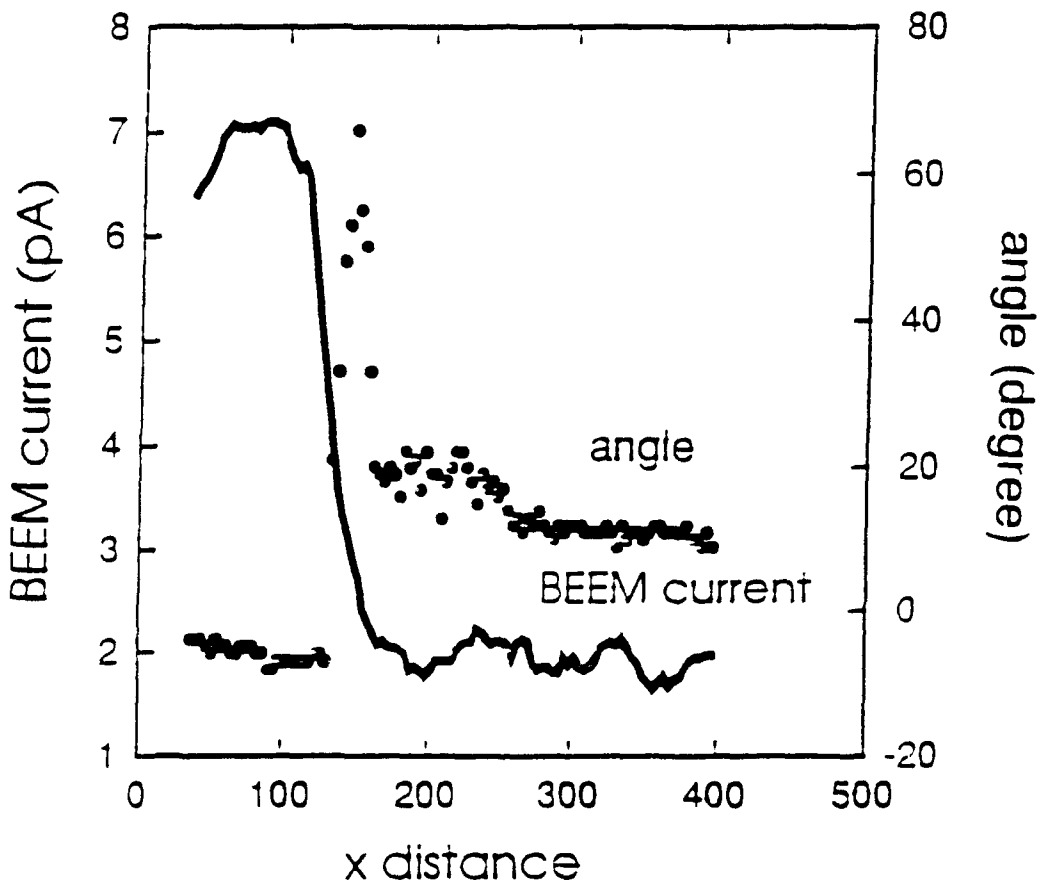
BEEM current (pA)
angle (degree)
x distance
angle
BEEM current
8
7
6
5
4
3
2
1
80
60
40
20
0
-20
0
100
200
300
400
500

Fig. 3

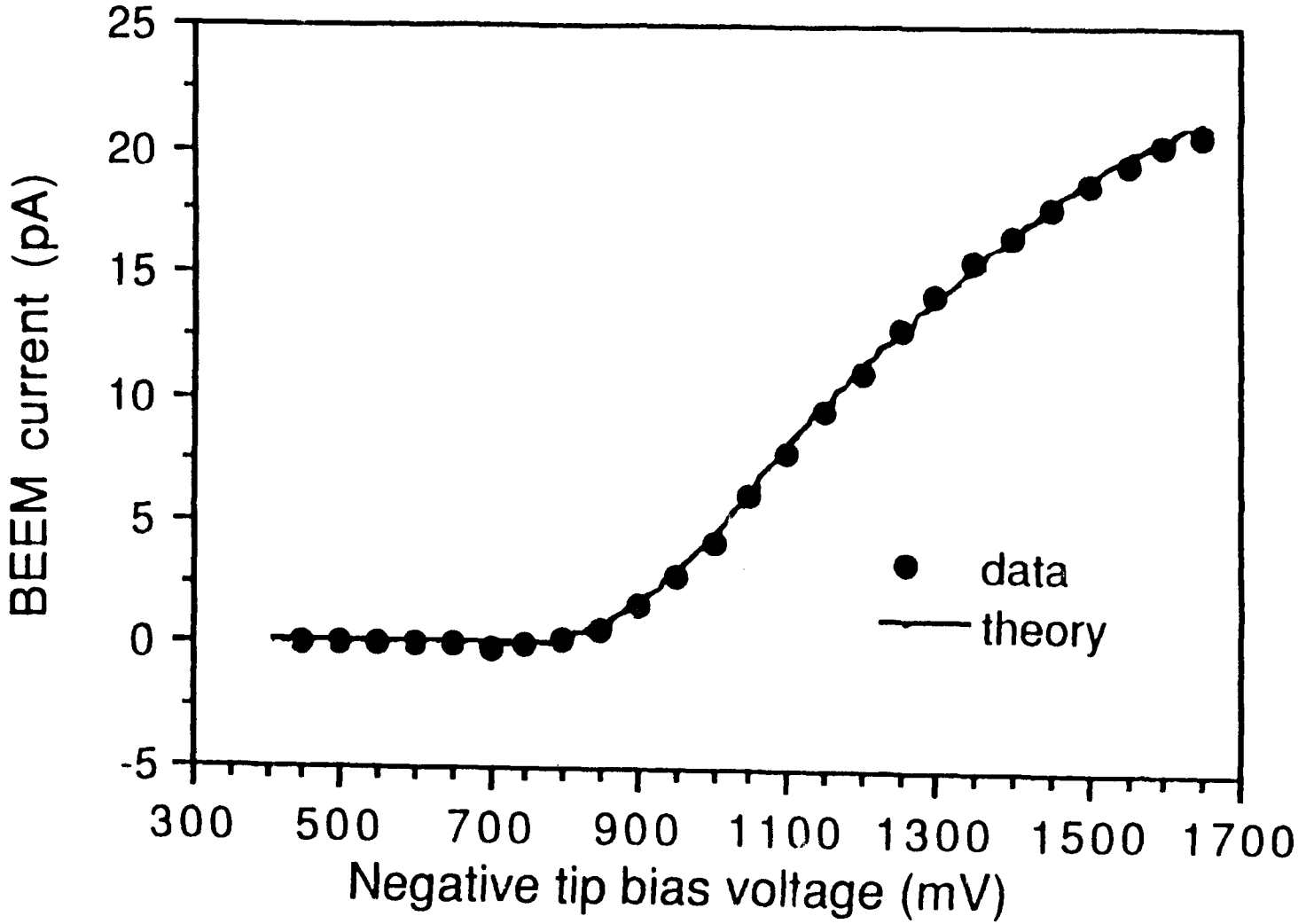
25
20
15
10
5
0
-5
BEEM current (pA)
300
500
700
900
1100
1300
1500
1700
Negative tip bias voltage (mV)
data
theory

Fig. 4

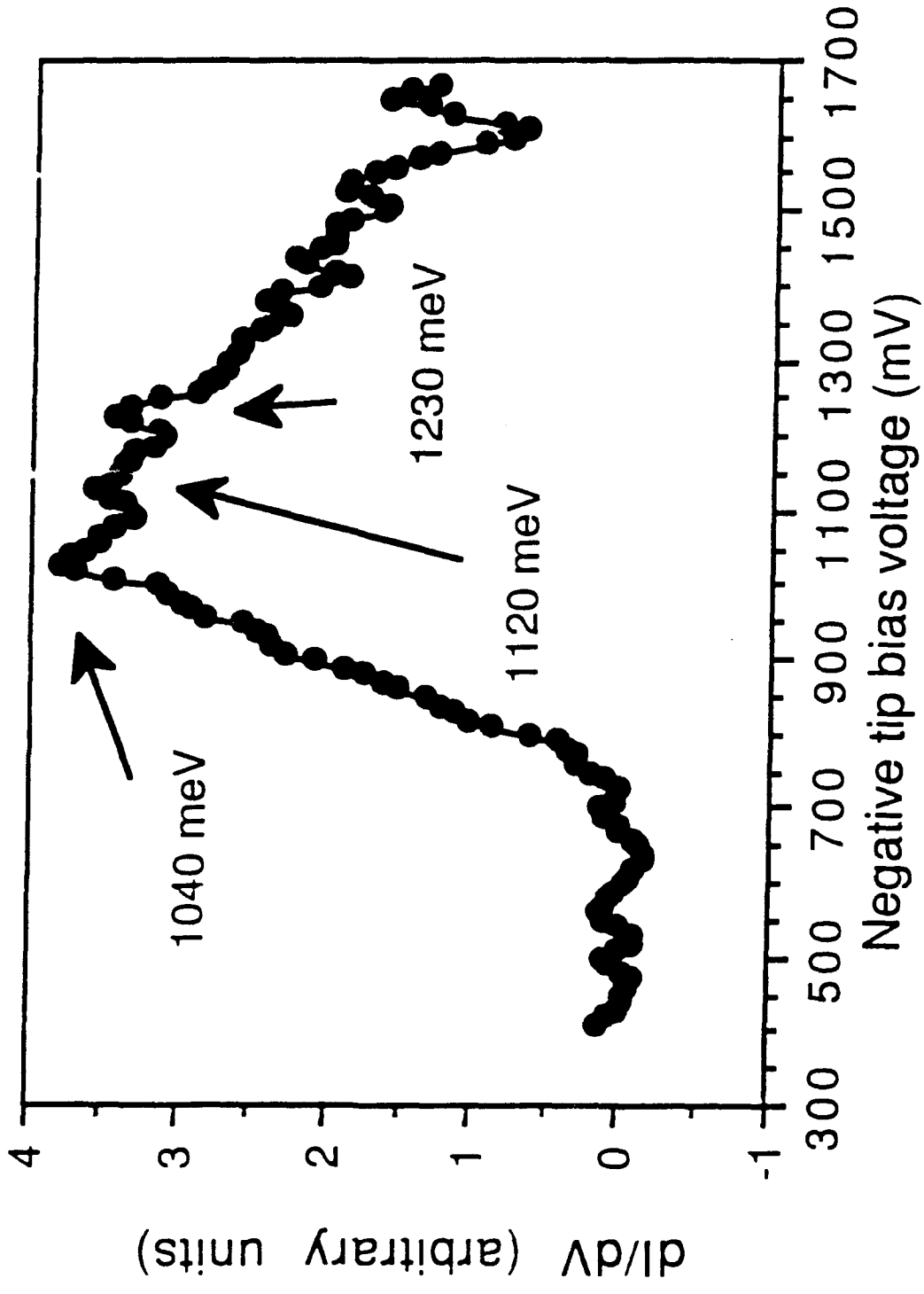
dI/dV (arbitrary units)
4
3
2
1
0
-1
300
500
700
900
1100
1300
1500
1700
Negative tip bias voltage (mV)
1040 meV
1120 meV
1230 meV

Fig. 5

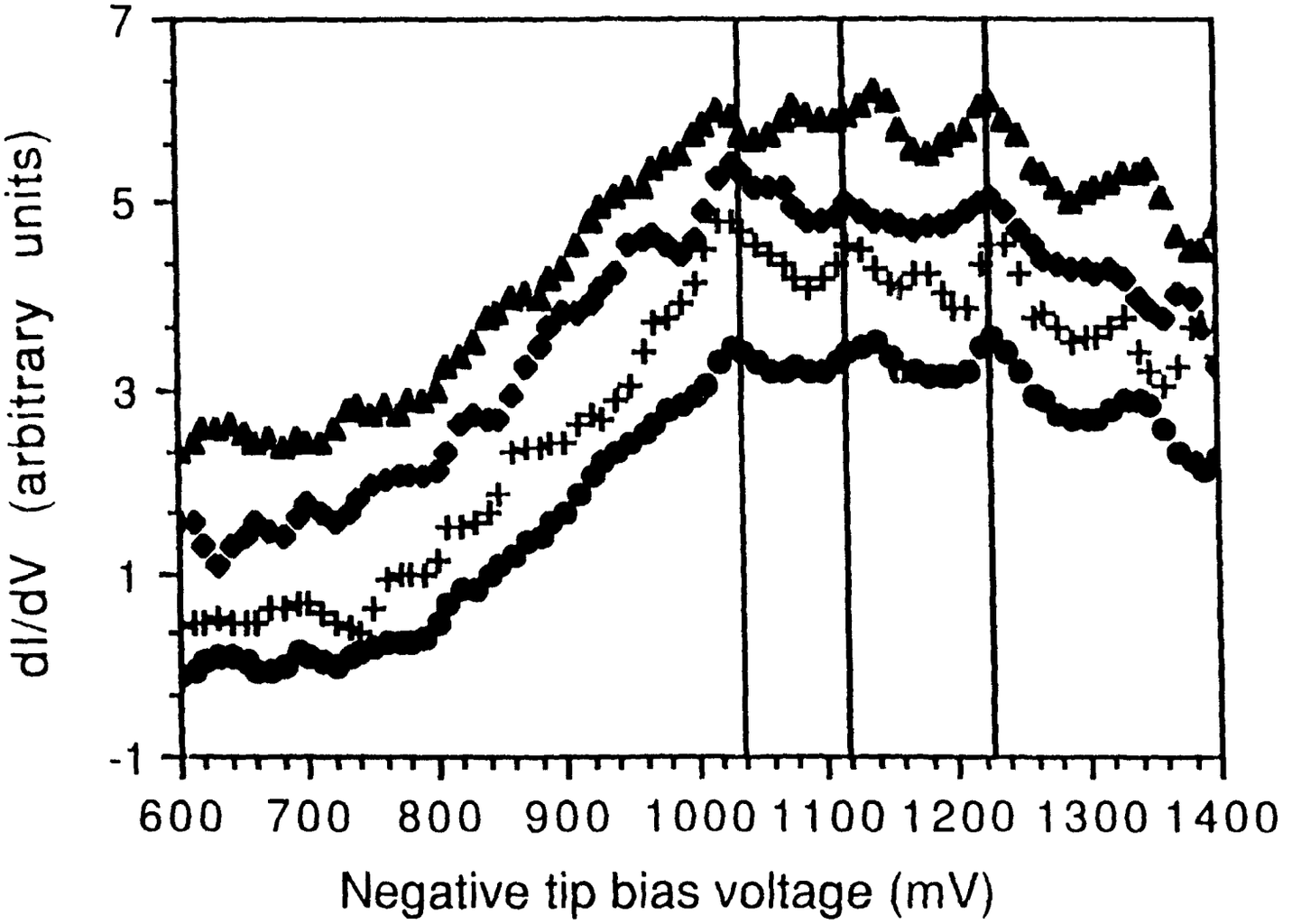
7
5
3
1
-1
dI/dV (arbitrary units)
600 700 800 900 1000 1100 1200 1300 1400
Negative tip bias voltage (mV)

Fig. 6

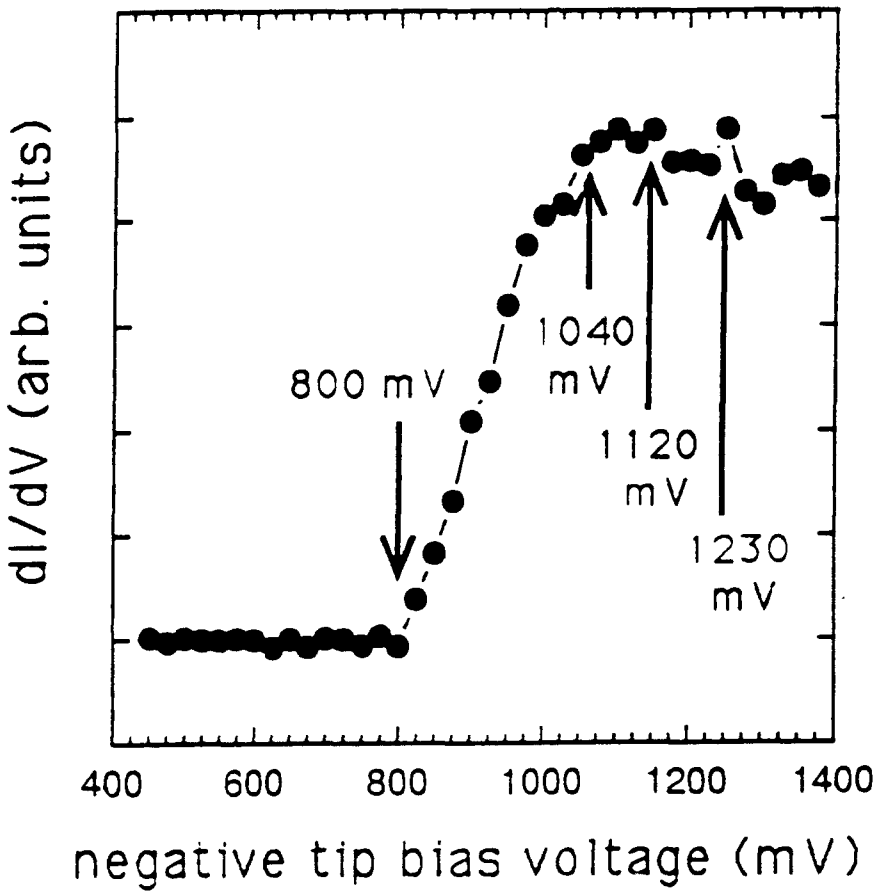
dI/dV (arb. units)
800 mV
1040 mV
1120 mV
1230 mV
400
600
800
1000
1200
1400
negative tip bias voltage (mV)

Fig. 7

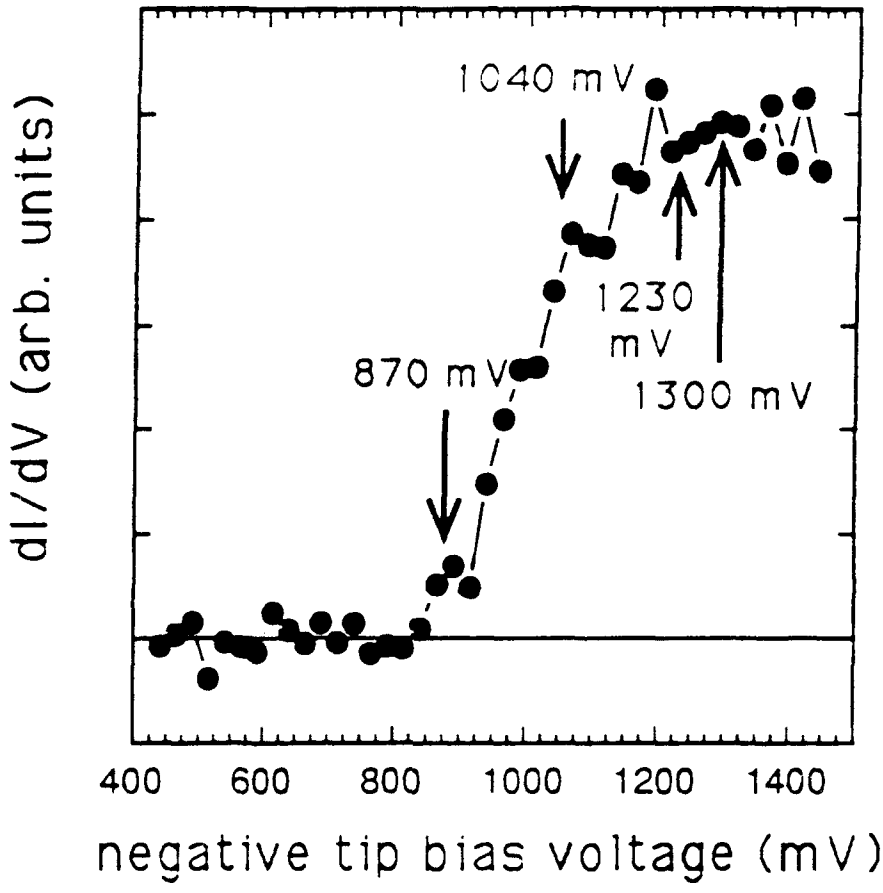
1040 mV
1230
mV
870 mV
1300 mV
dI/dV (arb. units)
400
600
800
1000
1200
1400
negative tip bias voltage (mV)

Fig. 8

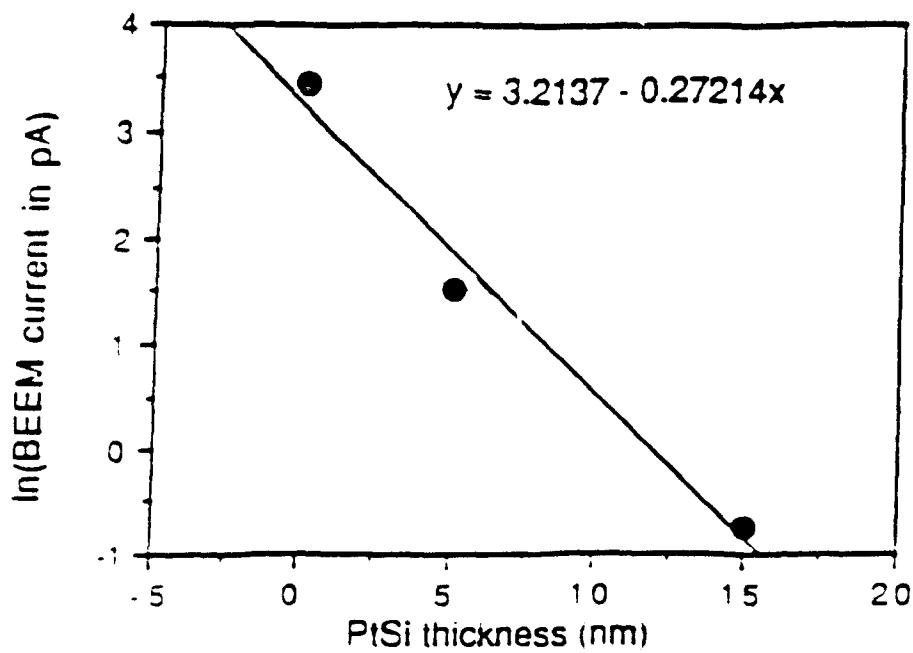
y = 3.2137 - 0.27214x
ln(BEEM current in pA)
PtSi thickness (nm)
4
3
2
1
0
-1
-5
0
5
10
15
20

Fig. 9

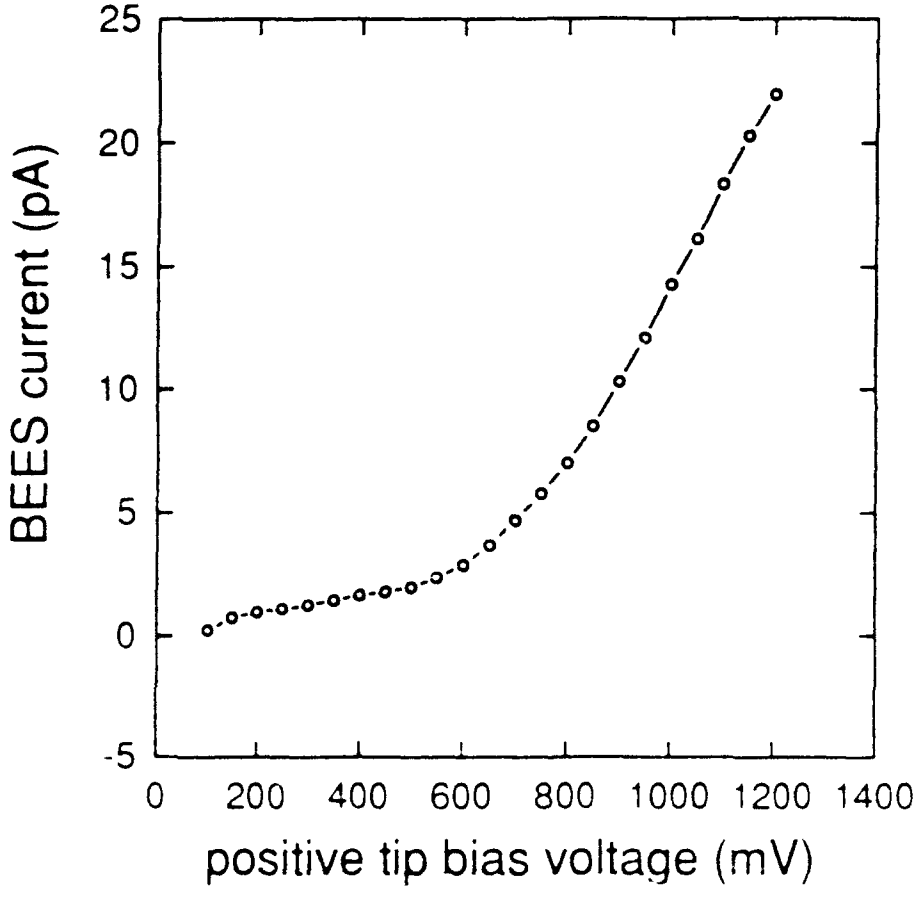
25
20
15
10
5
0
-5
BEES current (pA)
0
200
400
600
800
1000
1200
1400
positive tip bias voltage (mV)

Fig. 10

MISSION

OF

ROME LABORATORY

Rome Laboratory plans and executes an interdisciplinary program in research, development, test, and technology transition in support of Air Force Command, Control, Communications and Intelligence (C^3I) activities for all Air Force platforms. It also executes selected acquisition programs in several areas of expertise. Technical and engineering support within areas of competence is provided to ESD Program Offices (POs) and other ESD elements to perform effective acquisition of C^3I systems. In addition, Rome Laboratory's technology supports other AFSC Product Divisions, the Air Force user community, and other DOD and non-DOD agencies. Rome Laboratory maintains technical competence and research programs in areas including, but not limited to, communications, command and control, battle management, intelligence information processing, computational sciences and software producibility, wide area surveillance/sensors, signal processing, solid state sciences, photonics, electromagnetic technology, superconductivity, and electronic reliability/maintainability and testability.